



The structural connectome and motor recovery after stroke: predicting natural recovery

Philipp J. Koch,^{1,2,3} Chang-Hyun Park,^{1,2} Gabriel Girard,^{4,5,6} Elena Beanato,^{1,2} Philip Egger,^{1,2} Giorgia Giulia Evangelista,^{1,2} Jungsoo Lee,⁷ Maximilian J. Wessel,^{1,2} Takuya Morishita,^{1,2} Giacomo Koch,⁸ Jean-Philippe Thiran,^{4,5,6} Adrian G. Guggisberg,⁹ Charlotte Rosso,¹⁰ Yun-Hee Kim^{7,11} and Friedhelm C. Hummel^{1,2,12}

Stroke patients vary considerably in terms of outcomes: some patients present ‘natural’ recovery proportional to their initial impairment (fitters), while others do not (non-fitters). Thus, a key challenge in stroke rehabilitation is to identify individual recovery potential to make personalized decisions for neuro-rehabilitation, obviating the ‘one-size-fits-all’ approach.

This goal requires (i) the prediction of individual courses of recovery in the acute stage; and (ii) an understanding of underlying neuronal network mechanisms. ‘Natural’ recovery is especially variable in severely impaired patients, underscoring the special clinical importance of prediction for this subgroup.

Fractional anisotropy connectomes based on individual tractography of 92 patients were analysed 2 weeks after stroke (TA) and their changes to 3 months after stroke (TC – TA). Motor impairment was assessed using the Fugl-Meyer Upper Extremity (FMUE) scale. Support vector machine classifiers were trained to separate patients with natural recovery from patients without natural recovery based on their whole-brain structural connectomes and to define their respective underlying network patterns, focusing on severely impaired patients (FMUE < 20). Prediction accuracies were cross-validated internally, in one independent dataset and generalized in two independent datasets.

The initial connectome 2 weeks after stroke was capable of segregating fitters from non-fitters, most importantly among severely impaired patients (TA: accuracy = 0.92, precision = 0.93). Secondary analyses studying recovery-relevant network characteristics based on the selected features revealed (i) relevant differences between networks contributing to recovery at 2 weeks and network changes over time (TC – TA); and (ii) network properties specific to severely impaired patients. Important features included the parietofrontal motor network including the intra-parietal sulcus, premotor and primary motor cortices and beyond them also attentional, somatosensory or multi-modal areas (e.g. the insula), strongly underscoring the importance of whole-brain connectome analyses for better predicting and understanding recovery from stroke.

Computational approaches based on structural connectomes allowed the individual prediction of natural recovery 2 weeks after stroke onset, especially in the difficult to predict group of severely impaired patients, and identified the relevant underlying neuronal networks. This information will permit patients to be stratified into different recovery groups in clinical settings and will pave the way towards personalized precision neurorehabilitative treatment.

1 Defitech Chair of Clinical Neuroengineering, Center for Neuroprosthetics (CNP) and Brain Mind Institute (BMI), Swiss Federal Institute of Technology (EPFL), 1202 Geneva, Switzerland

Received May 28, 2020. Revised November 11, 2020. Accepted December 14, 2020. Advance access publication July 8, 2021

© The Author(s) (2021). Published by Oxford University Press on behalf of the Guarantors of Brain.

This is an Open Access article distributed under the terms of the Creative Commons Attribution Non-Commercial License (<http://creativecommons.org/licenses/by-nc/4.0/>), which permits non-commercial re-use, distribution, and reproduction in any medium, provided the original work is properly cited. For commercial re-use, please contact journals.permissions@oup.com

- 2 Defitech Chair of Clinical Neuroengineering, Center for Neuroprosthetics (CNP) and Brain Mind Institute (BMI), Swiss Federal Institute of Technology (EPFL Valais), Clinique Romande de Réadaptation, 1951 Sion, Switzerland
- 3 Department of Neurology, University of Lübeck, 23562 Lübeck, Germany
- 4 Signal Processing Laboratory (LTS5), School of Engineering, École Polytechnique Fédérale de Lausanne, CH-1015, Lausanne, Switzerland
- 5 Radiology Department, Centre Hospitalier Universitaire Vaudois and University of Lausanne, CH-1011, Lausanne, Switzerland
- 6 CIBM Center for BioMedical Imaging, CH-1015, Lausanne, Switzerland
- 7 Department of Physical and Rehabilitation Medicine, Center for Prevention and Rehabilitation, Heart Vascular Stroke Institute, Samsung Medical Center, Sungkyunkwan University School of Medicine, 06351 Seoul, Republic of Korea
- 8 Non Invasive Brain Stimulation Unit, Department of Behavioral and Clinical Neurology, Santa Lucia Foundation IRCCS, 00179 Rome, Italy
- 9 Division of Neurorehabilitation, Department of Clinical Neurosciences, Geneva University Hospitals, 1205 Geneva, Switzerland
- 10 Inserm U 1127, CNRS UMR 7225, Sorbonne Universités, UPMC Univ Paris 06 UMR S 10 27, Institut du Cerveau et de la Moelle épinière, ICM, France; AP-HP, Stroke Unit, Pitié-Salpêtrière Hospital, 75013 Paris, France
- 11 Department of Health Sciences and Technology, Department of Medical Device Management and Research, Department of Digital Health, SAIHST, Sungkyunkwan University, Seoul, Republic of Korea
- 12 Clinical Neuroscience, University of Geneva Medical School, 1202 Geneva, Switzerland

Correspondence to: Prof Dr Friedhelm Hummel
 Defitech Chair of Clinical Neuroengineering
 Center for Neuroprosthetics (CNP) and Brain Mind Institute (BMI)
 Swiss Federal Institute of Technology (EPFL), 9, Chemin des Mines
 1202 Geneva, Switzerland
 E-mail: friedhelm.hummel@epfl.ch

Correspondence may also be addressed to: Prof Yun-Hee Kim
 Department of Physical and Rehabilitation Medicine, Center for Prevention and Rehabilitation
 Heart Vascular Stroke Institute, Samsung Medical Center
 Sungkyunkwan University School of Medicine, 81 Irwon-ro Gangnam-gu
 Seoul 135-710, Republic of Korea
 E-mail: yun1225.kim@samsung.com or yunkim@skku.edu

Keywords: structural; connectivity; diffusion; stroke; recovery

Abbreviations: CST = corticospinal tract; FA = fractional anisotropy; FMUE = Fugl-Meyer Upper Extremity Scale; SVM = support vector machine; TA = 2 weeks after stroke; TC = 3 months after stroke

Introduction

Stroke is a leading cause of long-term disability, with > 1.5 million new cases each year in Europe; under 15% of the patients achieve full recovery, leaving 3.7 million patients with persistent impairment.¹ A significant remaining challenge is the heterogeneity in outcome and individual recovery potential and in the optimal neurorehabilitative strategy to maximize individual treatment outcome. To address these challenges in daily clinical practice, it is necessary to enhance the understanding and prediction of the individual courses of recovery. The identification of biomarkers of neuronal mechanisms, supporting the prediction of individual courses of recovery in an early phase, will have a massive impact on clinical management, translational research, and treatment choice in the pursuit of personalized precision medicine and will ultimately help to enhance patients' quality of life through its influences on healthcare systems and socioeconomics.^{2,3}

Regarding motor recovery after stroke, two phenomena have been suggested to represent key factors. First, a considerable proportion of patients (2/3) show natural improvement of ~70% of

their initial impairment^{4,5}; this recovery is supported by key mechanisms of intrinsic neuronal plasticity (spontaneous biological recovery), one possible key target for future therapies. The remaining patients (1/3) show considerably less natural (proportional) recovery and are defined herein as non-fitters. The mechanisms of intrinsic plasticity in these patients are altered or insufficient to lead to relevant natural recovery, strongly favouring the view that such patients need clearly alternative treatment strategies to maximize the outcome.

Second, for severely impaired patients, there is a large proportion of patients who do not show natural recovery.³ Individually identifying severely impaired patients, who will or will not show natural relevant recovery will have tremendous importance for treatment selection in the pursuit of precision therapy, but current literature and clinical work lack efforts to make these predictions.

Different systems neuroscience techniques,⁶ such as electrophysiology,^{7,8} diffusion weighted imaging,^{9–12} structural,¹³ and functional imaging,^{14,15} as well as first computational analytical approaches (e.g. machine learning), have been used in efforts to predict residual motor function¹⁶ or recovery.¹⁷ For instance, markers of corticospinal tract

(CST) integrity have been introduced in an attempt to distinguish patients with and without motor recovery.^{9,10} Nevertheless, most of the studies considered measures derived from focal brain regions, such as sensorimotor areas, although there is increasing evidence that stroke is a large-scale network disorder beyond the lesioned region itself, clearly showing the involvement of widely distributed areas and large-scale networks, of which nodes and edges might serve as a conjunct prediction matrix and provide specific targets for therapy (e.g. brain stimulation) for individual patients.^{18,19} Furthermore, prediction models so far have mainly neglected severely impaired patients, for which there is a strong need to stratify treatment options.

Connectome-based predictive modelling is a novel, exciting data-driven approach taking advantage of technical advances in reconstructing the whole-brain connectome from neuroimaging data; this type of predictive modelling has been successfully adapted to clinical problems.²⁰ Using whole-brain connectomes has the potential to identify neuronal networks underlying the recovery process and therefore provides valuable information towards individualized targets for new therapeutic strategies.

As the network properties supporting recovery are not static but dynamic over time, it becomes obvious that predictive network (re)organization supporting recovery might be different in the first weeks compared to months after stroke, adding a further dimension to the analyses (for a review, see Koch and Hummel¹⁹).

Overall, in a large sample of stroke patients, multimodal analyses of the structural connectome 2 weeks after stroke were used as a potential prognostic factor to determine individual outcome after stroke (recovery and no recovery) using computational approaches based on support vector machines (SVM). After developing and training of the prediction model, we validated the generated model first internally, then in an independent dataset externally; to then generalize it to general motor functions internally as well as within two independent datasets.

In secondary analyses, longitudinal connectome changes 2 weeks to 3 months were leveraged in a similar fashion to define white matter changes supporting recovery and compared them with the 2 weeks connectomes. Additionally, we investigated how functional (motor, sensory and attention) systems of the connectome contribute differently to the prediction. The predictive accuracy was compared to the CST and other measurements of neural networks, and we analysed the long-term changes in local diffusivity relevant for functional recovery. The study was especially focused on severely impaired patients.

Material and methods

Datasets

Three independent datasets were collected. The first dataset, referred to as the SEOUL dataset was used for training and internal validation, whereas the second (GENEVA) was used for the external validation of the trained models and the third dataset (PARIS) was used for the generalization of the proportional recovery-based prediction to other motor recovery measures.

All patients were evaluated by imaging and motor function evaluation. For SEOUL, 63 patients after stroke (58 ± 12.6 years old, 33 male) were assessed 2 weeks (14.6 ± 6.6 days) and 3 months (98.3 ± 12.6 days) after stroke onset. Motor function was evaluated by means of the Fugl-Meyer score of the upper extremity (FMUE), grip strength, pinch grip strength and box and block test.

For the first validation (GENEVA), 15 patients were recruited (58 ± 12.2 years old, nine males), and evaluated 2 weeks after stroke (TA, 18.3 ± 9.1 days). For 10 of those patients a second evaluation at

3 months was performed (TC, 113.6 ± 34.4 days). Motor function was evaluated by means of the FMUE and grip strength.

For the second validation (PARIS) 14 patients (55 ± 16.7 years old, nine males) were evaluated 4 weeks (TA, 28.6 ± 7.2 days) and 3 months (TC, 90.4 ± 12.7 days) after stroke. Motor function was evaluated by means of grip strength.

Inclusion criteria were first-ever ischaemic stroke, ≥ 18 years old, and absence of other neuropsychiatric or life-threatening comorbidities.

The study was approved by local ethic committees at each site. Written informed consent was obtained from each participant according to the Declaration of Helsinki.

Data acquisition

SEOUL dataset

All images for the training and testing dataset were acquired using a 3T Philips ACHIEVA MRI scanner (Philips Medical Systems). High-resolution T_1 -weighted anatomic images were acquired using a 3D magnetization-prepared, rapid acquisition gradient-echo sequence (MPRAGE) with the following parameters: 124 axial slices, slice thickness = 1.6 mm, no gap, matrix size 512×512 , field of view 240×240 . For the diffusion-weighted images diffusion gradients with a b-value of 1000 s/mm^2 single shell were obtained in 45 non-collinear directions covering the whole brain in 75 axial slices. The following acquisition parameters were used: repetition time = 8770 ms, echo time = 60 ms, field of view = 220×220 mm, slice thickness = 2.25 mm, in-plane resolution = 1.96×1.96 mm.

GENEVA dataset

All images for the training and testing dataset were acquired using a 3T Siemens TRIO MRI scanner. High-resolution T_1 -weighted anatomic images were acquired using a 3D MPRAGE with the following parameters: 176 axial slices, slice thickness = 1.0 mm, matrix size 240×256 . For the diffusion-weighted images diffusion gradients with a b-value of 1000 s/mm^2 single shell were obtained in 30 gradient encoded directions covering the whole brain in 60 axial slices. The following acquisition parameters were used: repetition time = 7400 ms, echo time = 84 ms, field of view = 256×256 mm, slice thickness = 2 mm, in-plane resolution = 2×2 mm.

PARIS dataset

All images for the training and testing dataset were acquired using a 3T Siemens TRIO MRI scanner. High-resolution T_1 -weighted anatomic images were acquired using a 3D MPRAGE with the following parameters: 176 axial slices, slice thickness = 1.0 mm, matrix size 240×256 . For the diffusion-weighted images diffusion gradients with a b-value of 1000 s/mm^2 single shell were obtained in 35 gradient encoded directions covering the whole brain in 60 axial slices. The following acquisition parameters were used: repetition time = 10 s, echo time = 87 ms, field of view = 256×256 mm, slice thickness = 2 mm, in-plane resolution = 2×2 mm.

Data processing

Stroke lesions were manually drawn on the high resolution T_1 MPRAGE by a physician (P.K.) using mrview by mrtrix (<https://www.mrtrix.org/>) and independently validated by another experienced physician, interrater reliability was 95%. Structural images were preprocessed by means of the Freesurfer toolbox (<https://surfer.nmr.mgh.harvard.edu/>). This includes artefact corrections, transformation of the native space into the Talairach, normalization, skull strip, segmentation and registration. The Destrieux atlas was used for further cortical parcellations.²¹

The areas covering the central sulcus, being the pre- (M1) and postcentral (S1) gyrus as well as the precentral sulcus for the premotor cortex (PMC) were split in an anterior and posterior part along the whole extent of the respective mask using an in-house calculation using MATLAB (Mathworks, Natick, MA, USA). By combining resulting segmentations specific masks for M1, S1 and PMC were generated. Furthermore, to increase the dimensionality of the parcellation, each mask of the Destrieux atlas was split into a fixed number of parcellations along the longest axis, using FreeSurfer. Finally, we included subcortical areas as well as the cerebellum resulting in a whole brain parcellation of 333 areas of interest. In case of stroke lesions affecting the performance of parcellation, the correspondence part of the lesion on the unaffected hemisphere was used and interpolated over the lesioned brain as a brain transplant and fed into the above-described structural imaging processing. Structural parcellation was registered to the non-weighted (b0) diffusion acquisition using `flirt` and `fnirt` by `fsl` (<https://fsl.fmrib.ox.ac.uk/fsl/fslwiki>).

The diffusion images were preprocessed using `eddy`,²² including motion artefact reduction, correction for field inhomogeneity and eddy currents. Diffusion tensors were estimated alongside the corresponding fractional anisotropy (FA) map.²³ Constrained spherical deconvolution was used to estimate the fibre orientation distributions within each voxel. Whole brain probabilistic tractography calculated streamline estimates using second order integration over fibre orientation distribution (iFOD2) using 10 million streamlines.²⁴ For the origin of streamlines, individual white matter masks were chosen. Following further selection of one million streamlines based on white matter regions of interest, every streamline was weighted fitting the underlying diffusion signal based on the Stick and Ball model using `COMMIT`.²⁵ The mean FA over each streamline was calculated integrating the `COMMIT` weights. Whole brain connectomes were calculated based on the mean FA and 333 regions of interest. The diagonal of connectomes was then set to 0 as well as connections between areas of the same initial Destrieux parcellation.

Proportional recovery

Proportional recovery for patients was calculated as follows: the change in FMUE over time was related to the maximal amount of potential recovery [(FMUE at 3 months – FMUE at 2 weeks) / (66 – FMUE at 2 weeks)]. This observed proportional recovery was related to the predicted proportional recovery [0.7 (66 – FMUE_{TA}) + 0.4], as previously described.²⁶ By means of k-means clustering, patients were identified as fitters, i.e. revealing a proportional recovery, and non-fitters, i.e. patients lacking proportional recovery. Patients were further separated into severely impaired patients as previously described in Fugl-Meyer et al.²⁷ (≤ 20 FMUE at 2 weeks).

To address potential spurious correlations of the proportional recovery, further correlation analyses between initial severity and outcome, as well as recovery rate, were performed using a linear regression model, exploring potential biases as suggested by Hope et al.²⁸

Application of machine learning classifiers

FA values of white matter tracts between 333 regions were used as features for classifying patients into fitters and non-fitters. We considered different classification tasks according to the inclusion of time points and the severity of patients' initial motor impairment. That is, different machine learning classifiers were constructed according to (i) whether FA values at 2 weeks (i.e. TA) or changes in FA values between 2 weeks and 3 months (i.e. TC – TA) were used as features; and (ii) whether all patients or subgroup

patients with severe initial motor impairment were included as instances. For the classification tasks, an SVM was used as a machine learning method.

The SEOUL dataset was used to train SVM classifiers for the classification tasks. Features were adjusted for effects of patients' age, lesion affecting dominant or non-dominant hemisphere, NIH Stroke Scale (NIHSS) scores at TA, and initial lesion volume by obtaining residuals after regressing out the confounding covariates. We selected a feature subset to reduce the risk of overfitting by filtering features via a two-sample t-test between fitters and non-fitters with the significance level of a P-value ≤ 0.05 or less uncorrected for multiple comparisons. SVM classifiers were trained for the selected features by tuning hyperparameters including box constraint and kernel scale via 5-fold cross-validation. Kernel function was fixed to using the linear kernel since we were interested in assessing the importance of individual features in terms of their SVM classifier weights. The performance of SVM classifiers was evaluated in terms of classification accuracy and precision firstly using the SEOUL dataset in 5-fold cross-validation as internal validation and secondly using the GENEVA dataset as external validation.

In addition, to distinguish features specific to a subgroup, patients with severe initial motor impairment, we performed 10 000 times of permutation by which patients' labels based on the severity of their initial motor impairment were ordered randomly. For the subgroup of patients with severe initial motor impairment, we compared the feature subset determined for actual labels in relation to the distribution of feature subsets determined for permuted labels. We supposed that a lower selection frequency of a feature in the distribution (<5%) could indicate its greater specificity to the subgroup of patients with severe initial motor impairment compared to all patients.

Feature extraction

For every parcellation of the brain (nodes), weights of all connections to this area included as a feature in the SVM (surviving the two-sample t-test) were summed up. A high value of a node thereby indicates this brain area has multiple connections for which a higher FA or change in FA indicates a higher likelihood of the patient being a fitter. A lower value of a node indicates that this brain area has multiple connections for which a higher FA or change in FA indicates a higher likelihood of being a non-fitter. This procedure was repeated for all trained and tested SVM classifiers using the connectome at TA and the changes over time for both the whole SEOUL dataset as well as the subgroup of patients with initial severe impairment. Values for the nodes were z-transformed and visualized on the inflated FreeSurfer surfaces as well as MNI standard brain showing only positive and negative values \pm one standard deviation (SD) (Fig. 2 and Supplementary Figs 1–4).

Generalization

We assessed whether SVM classifiers are relevant to motor recovery measures other than fitter versus non-fitter classification. A function that transformed SVM classification scores to posterior probabilities was estimated, such that a higher posterior probability indicated a higher likelihood of being classified as a fitter. We considered correlations with two additional motor recovery measures, namely, normalized changes in hand grip strength and principal component motor scores extracted from changes in hand grip strength, pinch grip strength, and box and block test scores. Statistical significance was determined at a P-value of 0.05.

Longitudinal change of the white matter microstructural integrity

For each connection of the connectome, FA values were compared between TA and TC using a paired dependent t-test. Those connections were considered for further analyses, which indicate a change of FA applying a significance level of 0.05 uncorrected for multiple comparison and additionally were included as a feature in the SVM classifier addressing the change of FA over time TC – TA. By this, surviving connections show (i) a change of FA over time; and (ii) a functional meaningful change of FA, by remaining vulnerable to type 1 errors. T-statistics for each connection were summed up for every area of the parcellation indicating brain areas, for which connections dominantly show an increase (negative values) or decrease (positive values) of FA over time. Additionally, positive and negative t-scores were summed for positive and negative features separately.

Contribution of functional networks

To compare the different contributions of functional networks and their interactions, areas belonging to either the motor, the somatosensory or the attention network were selected out of the 333 parcellations, as shown in [Supplementary Table 2](#). Note, that one area can be referred to more than one network. This selection was based on a literature review. In a stepwise approach, white matter connections of only the motor network (3081 connections) were used as features for classifying patients into fitters and non-fitters followed by white matter connections of the motor plus somatosensory system (9591 connections) followed by the motor plus somatosensory plus attentional system (13 203 connections) and finally the whole brain connectome (55 945 connections). For each step different machine learning classifiers were constructed for the FA at TA and changes in FA between TA and TC. All further steps were identical to the previous construction of SVM classifiers without external validation or permutation.

Comparison with CST integrity and network readouts

In order to relate connectome-based prediction accuracy to prediction models using different measures of network connectivity commonly used in literature, SVM classifiers were built based on the CST connectivity as well as network measurements by means of graph theory.

CST integrity was evaluated in two ways. A group average template of the trajectory of the CST from 842 healthy subjects from the Human Connectome Project was taken.²⁹ Individual FA maps were co-registered non-linearly to the Montreal Neurological Institute (MNI) standard space. FA values were read out in the trajectory of the CST template at the level from the mesencephalon to the cerebral peduncle (MNI coordinates $z = -25$ to $z = -20$) as suggested previously³⁰ reducing influence of crossing fibres. Second, the CST lesion load was calculated. Individually drawn lesion masks were non-linearly co-registered to MNI space. The volume overlay of the individual lesion mask and the CST group template was calculated.

These two values, in addition to the initial score of FMUE, were used as features to the SVM, classifying patients into fitters and non-fitters.

In addition, alternative SVM classifiers were constructed using seven network summary measures as features. Weighted structural networks were constructed by setting the 333 regions as nodes and using FA values of white matter tracts between them as edge weights. For constructed weighted structural networks, density as a size measure, characteristic path length as an integration measure, clustering coefficient as a segregation measure,³¹ participation

coefficient as a centrality measure, and assortativity,³² modularity,³³ and small-worldness³⁴ as structure measures were computed. Using the seven network measures as features, SVM classifiers were trained and tested for classifying fitters and non-fitters.

Data availability

Data will be made available upon reasonable request.

Results

Proportional recovery

The results of the clustering and identification of fitters and non-fitters for the SEOUL dataset is illustrated in [Fig. 1](#) and [Supplementary Table 1](#). Of all patients within the SEOUL dataset, 39.7% (25/63) were determined to be non-fitters, and in the subgroup with severe motor impairment, 63.9% (23/36) were identified as non-fitters. Segregating two clusters within the given dataset revealed more stable results compared to up to five clusters, as indicated by means of silhouette values ([Supplementary Figs 5 and 6](#)).

Potential biases of the proportional recovery model, like over-estimation or ceiling, were further investigated between initial severity and outcome/recovery, as well as ratio of variance, as suggested by Hope *et al.*²⁸ See [Table 1](#) for the respective results.

Classification performance internal validation: SEOUL dataset

[Table 2](#) displays the performance of SVM classifiers using initial FA values as features. First, SVM classifiers were cross-validated internally and yielded adequately high classification accuracy.

Using changes of FA values as features of internal validation yielded adequately high classification performance for all SEOUL patients (accuracy: 0.92; precision: 0.92), as well as for the severe patients in the SEOUL dataset (accuracy: 0.92; precision: 0.93).

Classification performance external validation: GENEVA dataset

Feature matrices extracted from the SVM classifier were additionally validated externally in the independent GENEVA dataset. Results for the initial FA values as features are shown in [Table 2](#). Note that the extreme classification accuracy of 1.0 in the external validation may be due to an imbalance within the GENEVA dataset, as all severe patients in the GENEVA dataset were identified as non-fitters and precision is depending on the recognition of fitters ([Supplementary Table 1](#)).

Using changes in FA values as features, external validation was carried out within the GENEVA dataset (accuracy: 0.6; precision: 0.6) and severe patients in the GENEVA dataset (accuracy: 1.0; precision: not applicable).

Generalization

To reveal whether extracted features were relevant not only for separating fitters and non-fitters but to further indicate changes in general motor recovery measures, posterior probability scores were correlated with scores of motor function within all datasets (SEOUL, GENEVA, PARIS). The results are presented in [Table 3](#).

Brain areas supporting the recovery process 2 weeks after stroke

Using feature extraction, we identified brain areas and their connections relevant to the recovery process at 2 weeks after stroke

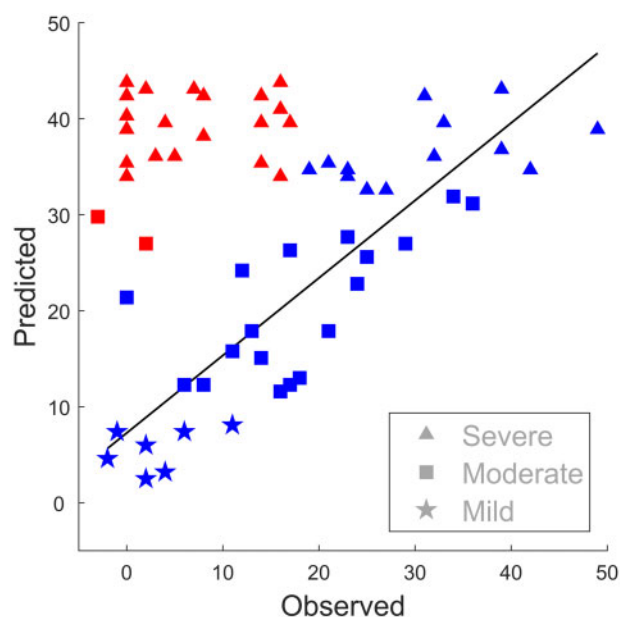


Figure 1 Fitters and non-fitters of proportional recovery. All patients in the SEOUL dataset are shown by their observed and predicted proportional recovery of FMUE. Non-fitters (red) are identified by the clustering showing less natural recovery than predicted [$0.7 (66 - \text{FMUE}_{\text{TA}}) + 0.4$] compared to the fitters (blue). For details, see the ‘Materials and methods’ section and [Supplementary Table 1](#).

for all patients, including severely impaired patients. The results are shown in [Fig. 2](#) and [Supplementary Figs 1 and 2](#). Descriptive analyses revealed that, on a cortical level, besides the involvement of bilateral motor cortices, bilateral involvement of connections with the ventral premotor cortex (PMv) (especially on the affected hemisphere) with involvement of further premotor areas like the inferior frontal gyrus is notable. Permutation analyses showed a specific supportive role of the PMv on the affected hemisphere in severely impaired patients ([Fig. 3](#)). In severely impaired patients specifically, is the relevant contribution of connections with the supplementary motor area (SMA) of the unaffected hemisphere.³⁵ Furthermore, there is a dominant role of connections within the parietal cortex including the intraparietal sulcus as well as the superior parietal gyrus on both hemispheres, with a specificity for severe patients (unaffected hemisphere).

Structural analyses further revealed that besides the areas of the core motor system, somatosensory or attentional regions, multimodal areas demonstrate relevant importance in separating fitters from non-fitters. In this regard, the relevance of the insular cortex, operculum, postcentral gyrus and cingulum (unaffected hemisphere) support the idea that higher residual structural connectivity of widespread networks involving multimodal areas is of obvious importance.

Finally, structural connectivity within subcortical structures also contributed to the prediction of proportional recovery, especially basal ganglia, thalamus and hippocampus, as well as projection fibres and cerebellar connections in severely impaired patients.

White matter changes supporting recovery between 2 weeks and 3 months after stroke

Longitudinal changes of structural connectivity after stroke and their relevance to proportional recovery were evaluated ([Fig. 2](#) and

[Supplementary Figs 3 and 4](#)). Higher values indicate the functional importance of an increase of FA over time or less decrease for positive features. Similar to the residual status at 2 weeks, white matter changes in connections with subcortical structures including bilateral basal ganglia and thalamus as well as brainstem and the cerebellum (unaffected hemisphere) are related to proportional recovery, with additional specificity for severely impaired patients ([Fig. 3](#)).

On a cortical level, the spatial distribution of areas supporting recovery are significantly different compared to 2 weeks after stroke. The influence of connections is prominently within areas of the frontal and temporal lobe, mainly on the affected hemisphere. Hereby, PMC as well as SMA and even more frontal areas like the middle and inferior frontal gyrus of the affected hemisphere contribute with a noticeable specificity in severe patients ([Fig. 3](#)). The temporal lobe, the superior temporal gyrus including secondary somatosensory areas and the insula are also highlighted.

Longitudinal changes of white matter microstructural integrity

Summed t-scores for the changes of FA over time for relevant connections are illustrated in [Fig. 4](#). For a detailed list of areas and t-scores, see [Supplementary Table 5](#).

The comparison between positive and negative features and t-scores revealed the following: 62 connections were negative features with a positive t-score and a summed value of 146.85, which indicates a decrease of FA over time correlating with a higher likelihood of being non-fitter. Four connections were negative features with a negative t-score and a summed value of 9.95, indicating an increase of FA over time with a higher likelihood of being non-fitter. Sixty-five connections were positive features with a positive t-score and a summed value of 162.32, indicating a decrease of FA, which correlates with higher likelihood of being a fitter, 25 connections were positive features with a negative t-score and a summed value of 57.66, indicating an increase of FA over time with a higher likelihood of being a fitter.

Contribution of functional networks

The accuracy and precision values determined by cross-validation of SVM classifiers using (i) only nodes considered to belong to the motor system; (ii) the previous nodes as well as nodes of the somatosensory system; (iii) the previous nodes as well as nodes of the attentional system; or (iv) the whole connectome, are shown in [Table 4](#). Using all subjects in the SEOUL dataset, the highest performance, as defined by accuracy and precision, was achieved using the motor and sensory functional nodes at 2 weeks (accuracy: 0.87; precision: 0.91) and over time (accuracy: 0.89; precision: 0.98).

For severely impaired patients, at 2 weeks, the highest performance was achieved using the whole connectome (accuracy: 0.92, precision: 0.93). For the change in the connectome over time, the highest performance was reached by considering only motor and somatosensory nodes (accuracy: 0.94; precision: 0.97). For information on which areas of the brain parcellation were considered to belong to each functional network, see [Supplementary Table 2](#).

Comparison with CST integrity, network readouts and motor evoked potential status

Accuracy measurements following cross-validation of a trained and tested SVM classifier using structural measurements of CST

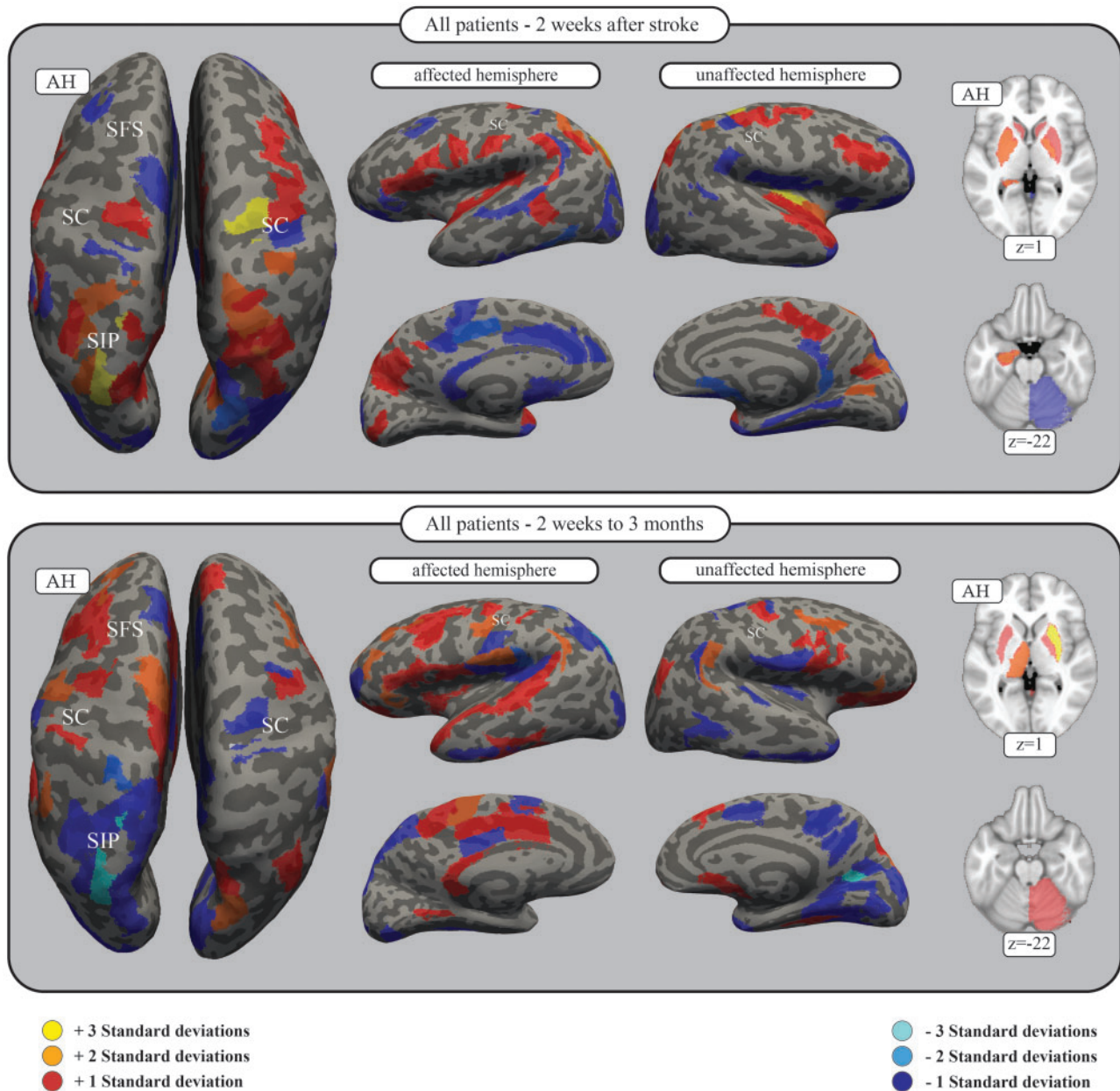


Figure 2 SVM features of all patients for connectomes 2 weeks after stroke as well as changes observed up to 3 months. Brain areas of the connectome in which connectivity positively (red) or negatively (blue) correlates with the likelihood of the patient being a fitter. The feature weights of all connections were summed for each area of the parcellation, and a z-transform was applied. Here, only those areas exceeding 1 SD are shown. For all results, see [Supplementary Table 4](#). The figure shows the results for the SVM including all subjects in the SEOUL dataset with the connectomes at 2 weeks after stroke (TA, top), as well as connectome changes to 3 months (TC – TA, bottom). The results are presented on the inflated FreeSurfer brain as well as the MNI standard brain, with z-coordinates given. Darker grey areas on the inflated FreeSurfer brain represent sulci, whereas lighter grey areas represent gyri. AH = affected hemisphere; SC = central sulcus; SFS = superior frontal sulcus; SIP = intraparietal sulcus.

integrity, like CST lesion load and FA together with the FMUE score at 2 weeks are shown in [Supplementary Table 9](#). Furthermore, results are presented when using predictors of network measure models including density, clustering coefficient, modularity, assortativity, characteristic path length, participation coefficient and small worldness. All models showed lower accuracy in predicting fitters versus non-fitters compared with the classifiers trained on the whole connectome.

Using motor evoked potential (MEP) data in 49 patients from the SEOUL dataset showed a 0.63 accuracy of predicting fitters and non-fitters in a confusion matrix ([Supplementary Table 7](#)). This

indicates a significantly lower predictive power than the current network connectomics approach.

Correlation between features at 2 weeks and changes between 2 weeks and 3 months after stroke

Regression analysis revealed a significant negative correlation between features at 2 weeks and features using connectome changes between 2 weeks and 3 months (coefficient: -0.14 , R^2 0.65, P -value < 0.0001). This correlation showed the same significant

Table 1 Correlation coefficients for the proportional recovery rule

X	Y	R ²	Coefficient	P	$\sigma(X)/\sigma(Y)$
FMUE TA	FMUE TC	0.608	0.86	<0.001	0.907
FMUE TA	FMUE rec	0.024	-0.14	0.116	1.420
FMUE TA (fitters)	FMUE TC (fitters)	0.479	0.37	<0.001	1.865
FMUE TA (fitters)	FMUE rec (fitters)	0.725	-0.63	<0.001	1.354
FMUE TA (severe)	FMUE TC (severe)	0.319	1.71	<0.001	0.331
FMUE TA (severe)	FMUE rec (severe)	0.074	0.71	0.108	0.386
FMUE TA (severe, fitters)	FMUE TC (severe, fitters)	0.001	0.06	0.907	0.621
FMUE TA (severe, fitters)	FMUE rec (severe, fitters)	0.256	-0.94	0.078	0.537

As suggested by Hope et al.,²⁸ we present correlation coefficients for $r(X, Y)$, $r(X, \Delta)$ as well as ratio of variance in X and Y for the FMUE scores at TA, TC and recovery scores.

Table 2 Internal and external validation performance of SVM classifiers

Patient subgroup	Feature set	Number of features	Accuracy	Precision
Internal validation (SEOUL dataset)				
All patients	Initial FA values (TA)	1765	0.83	0.87
Patients with severe initial motor impairment	Initial FA values (TA)	1921	0.92	0.93
External validation (GENEVA dataset)				
All patients	Initial FA values (TA)	1765	0.60	0.53
Patients with severe initial motor impairment	Initial FA values (TA)	1921	1.00	NA

Accuracy and precision estimated by cross-validation of SVM classifiers using the connectome at 2 weeks (TA) for both the whole SEOUL dataset and patients with severe initial motor impairment (internal validation). External validation was performed on an independent dataset (GENEVA). NA = not applicable.

Table 3 Generalization of features to further motor recovery scores

Patient group	Time point	Motor score	r	P
SEOUL (63 patients)	TA	Proportional recovery score	0.3	<0.001
	TC – TA		0.33	<0.001
SEOUL severe (36 patients)	TA		0.27	0.029
	TC – TA		0.31	0.01
SEOUL (63 patients)	TA	PCA composite score	0.23	<0.01
	TC – TA		0.2	0.024
SEOUL severe (36 patients)	TA		0.44	<0.001
	TC – TA		0.44	<0.001
SEOUL, GENEVA, PARIS (92 patients)	TA	Grip strength	0.21	<0.01
SEOUL, GENEVA, PARIS (87 patients)	TC – TA		0.23	<0.01

PCA composite scores were built based on measurements of hand grip strength, pinch grip strength, and box and block test scores. Grip strength was normalized to sex, age and hand dominance. Those variables were correlated with posterior probabilities of SVM classifiers.

relationship when considering summed values for each node (coefficient -0.28; R² 0.08; P-value < 0.0001).

Discussion

Structural connectome in the acute stage as a potential prognostic parameter for motor recovery following stroke

Identifying phenotypes of recovery trajectories and their unique neuronal fundaments was the main focus of this work. We believe that this is an essential prerequisite for the development of personalized precision medicine in stroke recovery and for maximization of individual outcomes by patient-tailored treatment strategies, including novel neurotechnologies such as non-invasive brain stimulation (NIBS).^{19,37,38}

The distinction between patients with or without natural (motor) recovery, i.e. fitters or non-fitters, has been reproduced multiple times^{4,5} and is also demonstrated in the present data (Fig. 1). For patient groups with severe initial impairment, in particular, there was a large diversity between patients showing recovery and patients that did not.

Predicting patients' potential outcomes has not been addressed in detail, especially for this particular subgroup. Recently multiple phenotypes of behavioural recovery have been separated highlighting the importance of predictive modelling and the strong need for understanding neuronal fundaments of recovery.⁴⁰ Previous prediction models have attempted to distinguish patients with favourable outcomes from those without, using electrophysiological or imaging readouts focused purely on the motor system (e.g. MEP or CST structural integrity) and reached an accuracy between 70 and 86%.^{13,15,16,37} However, these models have relevant limitations in correct phenotyping, especially for severely

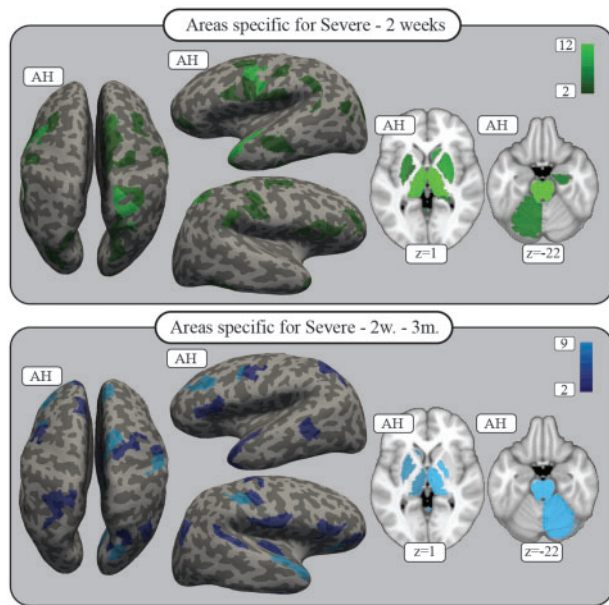


Figure 3 Permutation results, severe patients. The areas shown are those for which connectivity was specifically important for the distinction between fitters and non-fitters in the severely impaired patient group, as revealed by the permutation analyses for 2 weeks (top) as well as white matter change up to 3 months (bottom). The colour indicates how many connections for each area showed specificity. Areas with at least two specific connections are shown; all areas are plotted on the inflated FreeSurfer brain as well as the MNI standard brain with z-coordinates given. See [Supplementary Table 7](#) for the full results. AH = affected hemisphere.

impaired patients. Furthermore, the present approach takes into consideration the whole-brain connectome, which allows in-depth insight into neuronal networks involved in motor recovery beyond the CST and core motor areas.

Considering stroke as a network disorder and by applying SVM-based computational approaches to the whole-brain structural connectome, we were able to predict with high accuracy the fitter/non-fitter phenotype in the acute stage after stroke. It is notable that, for the first time, it was possible to accurately predict these phenotypes in severely impaired patients (e.g. severely impaired patients' TA connectome-based accuracy 0.92, precision: 0.93). It is important to note that, in addition to internal validation within the present dataset, the results were further validated in an independent, smaller dataset with a similar study design and imaging acquisition. The accuracy across all subjects reached 60%; however, the accuracy was 100% in severely impaired patients. Because the data sample was small, these validation results must be taken with caution, and more data are needed to validate the performance of the classification.

Finally, we were also interested in whether the used approach applied only to determine impairment as represented by the FMUE or also for residual motor function. To this end, we determined correlations between posterior probability and a composite motor score as well as normalized grip force. These analyses showed significance within the training dataset, as well as within the two validation datasets. This implies a generalizable meaning of the extracted features for recovery, not only in regard to impairment (FMUE), but also for pure residual motor functions (including distal skilled functions). Interestingly, this correlation showed higher coefficients for the group of severely impaired patients, indicating a higher generalizability of involved areas and networks for motor recovery for this patient group.

There is increasing focus on developing biomarkers for phenotyping and personalization of translational neuroscience, though the expression 'biomarker' is used frequently with different or un-specific definitions leading to a heterogeneous understanding of what is exactly meant. Prognostic biomarkers are used to indicate the likelihood of e.g. a disease's recurrence, measured at baseline in patients diagnosed with a certain disease, as defined by the FDA-NIH Biomarker Working Group.⁴¹ Because of the complexity of the most relevant neurological disorders, such as Alzheimer's or Parkinson's disease, multiple sclerosis or stroke, it has been a large challenge to identify prognostic biomarkers and bring them to the clinical domain.⁴²

Using an SVM model, 1765 features were extracted from the structural connectomes, assessed 2 weeks after the onset of an ischaemic stroke, predicting a favourable outcome 3 months after stroke with an accuracy of 83% (92% in severely impaired patients). For a high predictive performance on an individual basis, high values of area under the ROC curve (AUC) are one of the prerequisites; demonstrated here by an AUC of 0.957 (severe patients: 0.973) ([Supplementary Fig. 8](#)). The idea of using brain connectomics-based or other system neuroscience parameters combined with computational approaches might help in the development of novel biomarkers for complex neurological disorders, as previously suggested.⁴³ Further prospective clinical trials are needed to validate the medical utility of the structural connectome as a potential prognostic biomarker for natural motor recovery.

The proportional recovery model

Recently, the proportional recovery model has been challenged due to various confounds, namely mathematical coupling or ceiling,^{28,44} leading to a potential overestimation of the predictive value and explained variance. In particular, they point out the possibility of a spurious correlation between initial severity (X) and outcome (Y). Nevertheless, these analyses support the idea that there is a key fundamental difference between patients with natural recovery versus patients without natural recovery (Δ), i.e. fitters versus non-fitters, which was the main outcome variable in this analysis. However, overestimating the predicted proportional recovery within our subgroup may still influence the separation of patients into fitters or non-fitters on an individual level. To address this, further analyses, as suggested by Hope *et al.*,²⁸ have been performed and revealed (i) stronger correlations of initial impairment with recovery $r(X, \Delta)$ than with sole outcome $r(X, Y)$; (ii) an imbalance of variance towards outcome $[\sigma(X)/\sigma(Y)]$ within all patients, including the severely impaired; and (iii) strong prediction accuracy when removing mildly and moderately impaired patients. All in all, these points reduce the likelihood of false estimation and ceiling effects (see [Table 1](#) for the additional analyses).

Furthermore, clustering analyses with a lower (r : 0.6) or higher (r : 0.8) proportional recovery coefficient, as suggested, did not significantly affect the subgroups of fitters and non-fitters within the present cohort ([Supplementary Fig. 7](#)).

In summary, the analyses indicated stability within the segregation of fitters and non-fitters in the present data. Nevertheless, because of rising concerns with the proportional recovery model, there is a need for novel classifications of patients' recovery rates without these limitations.

The importance of networks in stroke

Using whole-brain structural connectomes for prediction further allows the determination of brain networks supporting or even hampering motor recovery. Using permutation and iteration methods, we were able to identify network nodes, which are

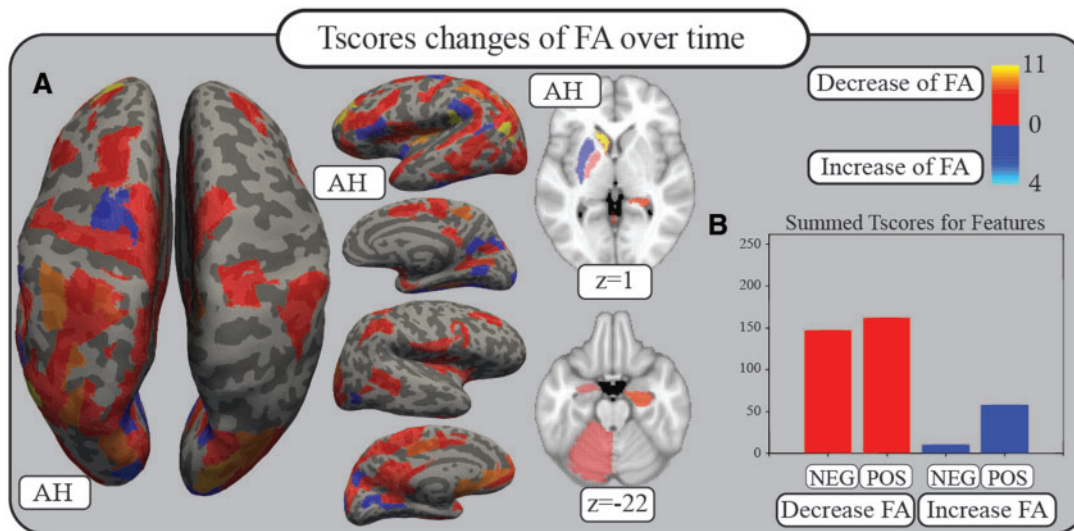


Figure 4 White matter changes. Comparison of the FA status of each connection relevant for recovery prediction (features) at 2 weeks compared to 3 months by Student's t-test reveals predominantly t-scores that show a decrease in FA (red). Blue colours indicate an increase in FA over time. Lacking correction for multiple comparisons, these results must be considered with caution. Numbers and colour codes represent the t-score. (A) Summed t-scores of features for each area are plotted on the inflated FreeSurfer cortex as well as the standard MNI brain with z-coordinates given. (B) Summed t-scores for weights that show a decrease or an increase in FA, separated between positive and negative features. AH = affected hemisphere; FA = fractional anisotropy; NEG = connections being negative features; POS = connections being positive features.

Table 4 Contributions of functional networks

	Accuracy				Precision			
	Motor	Motor + Sensory	Motor + Sensory + Attention	Whole	Motor	Motor + Sensory	Motor + Sensory + Attention	Whole
All 2 weeks	0.87	0.87	0.87	0.83	0.90	0.91	0.83	0.87
All 2 weeks to 3 months	0.81	0.89	0.86	0.92	0.82	0.98	0.87	0.92
Severe 2 weeks	0.83	0.89	0.83	0.92	0.83	0.85	0.97	0.93
Severe 2 weeks to 3 months	0.81	0.94	0.89	0.92	0.88	0.97	0.93	0.93

Accuracy and precision results measured by cross-validation of SVM classifiers consequently adding nodes of the structural connectome starting with the motor, sensory and attentional network. This was carried out for the entire SEOUL dataset as well as considering only patients with severe initial impairment.

especially important for recovery in severely impaired patients. We assumed that these brain areas are likely to underlie the processes of intrinsic neuronal plasticity (spontaneous biological recovery) and thereby could strongly influence the design of new therapeutic treatments, e.g. as multiple targets for NIBS.

Descriptive analyses of the importance of brain areas and their connections at 2 weeks following stroke revealed (Fig. 2) that connectivity within core parietofrontal motor areas, including primary motor, premotor cortices such as PMv, SMA and parietal areas (intraparietal sulcus and superior parietal gyrus), was crucial for favourable outcomes, supporting the literature emphasizing the importance of the parietofrontal network.^{30,37,44,45,47} Secondary motor areas were especially important in patients with severe initial impairment (Fig. 3). In addition to core motor areas, connections within the somatosensory, the attentional or multimodality network, such as the insular cortex, the operculum, postcentral gyrus and cingulum, showed significant relevance for natural recovery, implying that a much larger network, as previously thought, and beyond the core motor network may be involved in the process of spontaneous biological recovery of motor functions. This assumption is further supported by the fact that using this large-scale connectome as a predictive value showed much better results in separating fitters from non-fitters than using only the

CST or motor network readouts from graph theory within these data (Supplementary Table 4). Adding nodes beyond the core motor system increases the prediction performance (Supplementary Table 2). This is in contrast to current literature mainly focusing on the CST and core motor areas (for reviews, see Ward³ and Guggisberg et al.¹⁸).

Finally, structural connectivity not only between cortical areas, but also within subcortical structures was related to proportional recovery with high specificity in severely impaired patients, highlighting the relevant role of connections with subcortical structures and projection fibres for recovery.^{46,47}

The spatial patterns of areas relevant for prediction of outcome at 2 weeks overlapped to a certain degree with areas determined at the longitudinal changes, but they were clearly not identical, showing a shift towards a frontal and temporal representation (Figs 1 and 2 and Supplementary Figs 1–4). This strongly advocates that the pre-existing status of white matter connections (at 2 weeks) contributes differently to recovery than the network alterations (2 weeks to 3 months). More specifically, it is notable that for certain areas, e.g. the parietal cortex or the cingulum, the structural connectivity at 2 weeks clearly supported recovery; however, in contrast, a strengthening of this connectivity over time was rather disruptive for the recovery process. This implies that the functional importance of brain areas that show fast

and dynamic changes with time after stroke ranges from supporting to hampering recovery, pointing to a novel principle for neuronal correlates of motor recovery. Based on this, one could speculate that areas with connections of high integrity supporting recovery in an early phase are in need of reduction of input, whereas areas with a lower structural integrity are in need of strengthening their input with time for recovery, creating a more balanced and fine-tuned system that favours recovery. Future research is needed to confirm and deepen these conceptual aspects.

Finally, white matter connectivity features important for recovery were clearly different from those determining symptom severity at onset (2 weeks), as shown by comparison with a generated classifier separating severe versus moderate/mild initial impairment (Supplementary Table 8).

Changes in microstructure over time

Considering the massive, differential changes in the functional role of structural connections for recovery, it is crucial to determine by which microstructural means, by which ‘polarity’, they impact proportional recovery. Therefore, in both scenarios (i) a stronger increase in FA; and (ii) a smaller decrease in FA for a certain connection can determine the higher likelihood of being a fitter (for positive features) in the SVM classifier. As it is a matter of debate whether changes in white matter after stroke are more likely considered as degeneration or reorganization, both scenarios might be possible. To address this question, for every connection that showed differential relevance for the classification (feature extraction in the SVM), the FA status was compared between 2 weeks and 3 months (Fig. 4 and Supplementary Table 5). This analysis revealed that in a large number of these connections, a decrease in the mean FA was found, as well as a consistent pattern of area-specific decrease in FA—especially for the affected hemisphere. With due consideration for the lack of specificity of the microstructural readout used, these analyses point towards dominantly degenerative processes in white matter microstructural changes following stroke. Further investigation of white matter tissue using more complex modelling is required to assess the reduction of FA as degeneration or reorganization.⁴⁸

The importance of the planning and reliability of trials

As noted above, the possibility of classifying patients in this early stage will open up the opportunity for new personalized treatments. Knowledge of whether a patient belongs to the group of fitters or non-fitters has a relevant impact on the design of clinical studies in the field of neurorehabilitation. For instance, for fitters, an intervention must add to the natural improvement; however, for non-fitters, who show none or very limited natural recovery, all potential improvements are relevant. An example of the clinical relevance of identified phenotypes is that for fitters only, there was a significant relationship between the initial FMUE and the degree of improvement over time (Supplementary Table 3).

With the ability to identify fitters and non-fitters reliably and making use of the acute connectome as a potential prognostic biomarker, power calculations can become much more accurate, impacting the necessary sample sizes and anticipated effect sizes while enabling more homogenous data and better interpretation of study results; this ability will reduce the need for large sample sizes within clinical studies.

Limitations

The diffusion acquisition and analysis used implied limitations. First, tractography is a method vulnerable to false estimations, and further microstructural readouts are sensitive by multiple alterations of local diffusivity, which—taken together—might over- or underestimate structural connectivity between certain brain areas. This risk was addressed by fitting each streamline to the underlying diffusion signal using the COMMIT filtering method. Mechanistic conclusions about the underlying biological changes (e.g. differentiating myelin or axonal contribution) cannot be drawn confidently without more advanced acquisition (multi-shell), optimized filtering and complex microstructure. Second, stroke lesions affecting the cortex may influence cortical and whole brain structural reconstructions. Using the healthy hemisphere (for image transplant) may influence a bias not considering interhemispheric variability in structure. Third, the external validation dataset has a small sample size with an inhomogeneous distribution between the two classes of fitters and non-fitters, which led to unusual discrepancies in performance between internal and external validations. To facilitate the potential use of the predictive models at a single subject level, larger sample sizes are needed to further validate the performance of the prediction and thus its clinical usability. Lastly, the concept of proportional recovery has limitations, as pointed out and discussed above.

Summary

The presented analyses underscore the significant impact and high translational potential of computational analyses of whole-brain connectomes in predicting patients’ degree and course of recovery in an early stage following stroke. It provides the basis for clinically applicable biomarkers to classify patients, especially the group of severely impaired patients, for whom an accurate prediction has not been possible to reliably obtain thus far. Developing such prognostic biomarkers will help to stratify patient groups for precision therapy approaches and might guide clinical trials. The present data showed that areas beyond the core parietofrontal motor cortical network, such as the attentional, somatosensory or multimodal areas and subcortical structures, clearly contribute to the recovery process of motor functions and improve the classification. The pre-existing status of white matter connections in the acute stages contributes differently to recovery than the structural network alterations over time of the recovery phase.

Funding

Partially supported by #2017-205 ‘Personalized Health and Related Technologies (PHRT-205)’ of the ETH Domain, Defitech Foundation (Strike-the-Stroke project, Morges, Switzerland), Wyss Foundation (AVANCER WCP030, Genève, Switzerland), Bertarelli Foundation (Catalyst Deep-MCI-T project), National Research Foundation of Korea (NRF) grant (MSIP; NRF-2020R1A2C3010304). We acknowledge access to the facilities and expertise of the CIBM Center for Biomedical Imaging, a Swiss research center of excellence founded and supported by Lausanne University Hospital (CHUV), University of Lausanne (UNIL), Ecole polytechnique fédérale de Lausanne (EPFL), University of Geneva (UNIGE) and Geneva University Hospitals (HUG).

Competing interests

The authors report no competing interests.

Supplementary material

Supplementary material is available at *Brain* online.

References

- GBD 2016 Stroke Collaborators. Global, regional, and national burden of stroke, 1990–2016: a systematic analysis for the Global Burden of Disease Study 2016. *Lancet Neurol.* 2019;18(5):439–458.
- Stinear CM. Prediction of motor recovery after stroke: advances in biomarkers. *Lancet Neurol.* 2017;16:826–836.
- Ward NS. Restoring brain function after stroke – bridging the gap between animals and humans. *Nat Rev Neurol.* 2017;13:244–255.
- Stinear CM, Byblow WD, Ackerley SJ, Smith MC, Borges VM, Barber PA. Proportional motor recovery after stroke: Implications for trial design. *Stroke.* 2017;48:795–798.
- Winters C, van Wegen EEH, Daffertshofer A, Kwakkel G. Generalizability of the proportional recovery model for the upper extremity after an ischemic stroke. *Neurorehabil Neural Repair.* 2015;29:614–622.
- Kim B, Winstein CJ. Can neurological biomarkers of brain impairment be used to predict post-stroke motor recovery? A systematic review. *Neurorehabil Neural Repair.* 2017;31(1):3–24.
- Liuzzi G, Hörniß V, Lechner P, et al. Development of movement-related intracortical inhibition in acute to chronic subcortical stroke. *Neurology.* 2014;82:198–205.
- Nicolo P, Ptak R, Guggisberg AG. Variability of behavioural responses to transcranial magnetic stimulation: Origins and predictors. *Neuropsychol.* 2015;74:137–144.
- Buch ER, Rizk S, Nicolo P, Cohen LG, Schnider A, Guggisberg AG. Predicting motor improvement after stroke with clinical assessment and diffusion tensor imaging. *Neurology.* 2016;86:1924–1925.
- Byblow WD, Stinear CM, Barber PA, Petoe MA, Ackerley SJ. Proportional recovery after stroke depends on corticomotor integrity. *Ann Neurol.* 2015;78:848–859.
- Feng W, Wang J, Chhatbar PY, et al. Corticospinal tract lesion load: An imaging biomarker for stroke motor outcomes. *Ann Neurol.* 2015;78:860–870.
- Puig J, Blasco G, Schlaug G, et al. Diffusion tensor imaging as a prognostic biomarker for motor recovery and rehabilitation after stroke. *Neuroradiology.* 2017;59:343–351.
- Rondina JM, Filippone M, Girolami M, Ward NS. Decoding post-stroke motor function from structural brain imaging. *Neuroimage Clin.* 2016;12:372–380.
- Hannanu FF, Zeffiro TA, Lamalle L, et al. Parietal operculum and motor cortex activities predict motor recovery in moderate to severe stroke. *Neuroimage Clin.* 2017;14:518–529.
- Rehme AK, Volz LJ, Feis DL, Eickhoff SB, Fink GR, Grefkes C. Individual prediction of chronic motor outcome in the acute post-stroke stage: Behavioral parameters versus functional imaging. *Hum Brain Mapp.* 2015;36:4553–4565.
- Rehme AK, Volz LJ, Feis DL, et al. Identifying neuroimaging markers of motor disability in acute stroke by machine learning techniques. *Cereb Cortex.* 2015;25:3046–3056.
- Burke Quinlan E, Dodakian L, See J, et al. Neural function, injury, and stroke subtype predict treatment gains after stroke. *Ann Neurol.* 2015;77:132–145.
- Guggisberg AG, Koch PJ, Hummel FC, Buetefisch CM. Brain networks and their relevance for stroke rehabilitation. *Clin Neurophysiol.* 2019;130:1098–1124.
- Koch PJ, Hummel FC. Toward precision medicine: Tailoring interventional strategies based on noninvasive brain stimulation for motor recovery after stroke. *Curr Opin Neurol.* 2017;30:388–397.
- Shen X, Finn ES, Scheinost D, et al. Using connectome-based predictive modeling to predict individual behavior from brain connectivity. *Nat Protoc.* 2017;12:506–518.
- Destrieux C, Fischl B, Dale A, Halgren E. Automatic parcellation of human cortical gyri and sulci using standard anatomical nomenclature. *Neuroimage.* 2010;53:1–15.
- Andersson JLR, Sotiropoulos SN. An integrated approach to correction for off-resonance effects and subject movement in diffusion MR imaging. *Neuroimage.* 2016;125:1063–1078.
- Le Bihan D, Mangin J-F, Poupon C, et al. Diffusion tensor imaging: Concepts and applications. *J Magn Reson Imaging.* 2001;13:534–546.
- Tournier J-D, Smith R, Raffelt D, et al. MRtrix3: a fast, flexible and open software framework for medical image processing and visualisation. *Neuroimage.* 2019;202:116137.
- Daducci A, Dal Palù A, Lemkaddem A, Thiran JP. COMMIT: Convex optimization modeling for microstructure informed tractography. *IEEE Trans Med Imaging.* 2015;34:246–257.
- Prabhakaran S, Zahra E, Riley C, et al. Inter-individual variability in the capacity for motor recovery after ischemic stroke. *Neurorehabil Neural Repair.* 2008;22:64–71.
- Fugl-Meyer AR, Jääskö L, Leyman I, Olsson S, Steglind S. The post-stroke hemiplegic patient. 1. a method for evaluation of physical performance. *Scandinavian Journal of Rehabilitation Medicine.* 1975;7(1):13–31. 1135616
- Hope TMH, Friston K, Price CJ, Leff AP, Rotshtein P, Bowman H. Recovery after stroke: Not so proportional after all? *Brain.* 2019;142(1):15–22.
- Yeh FC, Panesar S, Fernandes D, et al. Population-averaged atlas of the macroscale human structural connectome and its network topology. *Neuroimage.* 2018;178:57–68.
- Schulz R, Koch P, Zimmerman M, et al. Parietofrontal motor pathways and their association with motor function after stroke. *Brain.* 2015;138(Pt 7):1949–1960.
- Watts DJ, Strogatz SH. Strogatz - small world network. *Nature.* 1998;393:440–442.
- Newman MEJ. Assortative Mixing in Networks. *Phys Rev Lett.* 2002;89:208701.
- Girvan M, Newman MEJ. Community structure in social and biological networks. *Proc Natl Acad Sci U S A.* 2002;99:7821–7826.
- Humphries MD, Gurney K. Network ‘Small-World-Ness’: A quantitative method for determining canonical network equivalence. *PLoS One.* 2008;3:e0002051.
- Quandt F, Bönstrup M, Schulz R, et al. The functional role of beta-oscillations in the supplementary motor area during reaching and grasping after stroke: A question of structural damage to the corticospinal tract. *Hum Brain Mapp.* 2019;40(10):3091–3101.
- Coscia M, Wessel MJ, Chaudary U, et al. Neurotechnology-aided interventions for upper limb motor rehabilitation in severe chronic stroke. *Brain.* 2019;142(8):2182–2197.
- Vliet R, Selles RW, Andrinopoulou E-R, et al. Recovery after stroke: A mixture model. 2020;87:383–393.
- Macgregor-Das A, Goggins M. Diagnostic biomarkers. In: *Pancreatic cancer.* Springer New York; 2018:659–680.
- Micera S, Caleo M, Chisari C, Hummel FC, Pedrocchi A. Advanced neurotechnologies for the restoration of motor function. *Neuron.* 2020;105(4):604–20.
- Mondello S, Salama MM, Mohamed WMY, Kobeissy FH. Editorial Biomarkers in neurology. *Front Neurol.* 2020;11:10–12.
- Kaiser M. The potential of the human connectome as a biomarker of brain disease. *Front Hum Neurosci.* 2013;7:1–4.

42. Hawe RL, Scott SH, Dukelow SP. Taking proportional out of stroke recovery. *Stroke*. 2019;50:204–211.
43. Rehme AK, Eickhoff SB, Wang LE, Fink GR, Grefkes C. Dynamic causal modeling of cortical activity from the acute to the chronic stage after stroke. *Neuroimage*. 2011;55:1147–1158.
44. Schulz R, Park E, Lee J, et al. Interactions between the corticospinal tract and premotor-motor pathways for residual motor output after stroke. *Stroke*. 2017;48:2805–2811.
45. Lindenberg R, Renga V, Zhu LL, Betzler F, Alsop D, Schlaug G. Structural integrity of corticospinal motor fibers predicts motor impairment in chronic stroke. *Neurology*. 2010;74:280–287.
46. Schulz R, Park E, Lee J, et al. Synergistic but independent: The role of corticospinal and alternate motor fibers for residual motor output after stroke. *NeuroImage Clin*. 2017;15:118–124.
47. Novikov DS, Veraart J, Jelescu IO, Fieremans E. Rotationally-invariant mapping of scalar and orientational metrics of neuronal microstructure with diffusion MRI. *Neuroimage*. 2018;174:518–538.
48. Bönstrup M, Schulz R, Schön G, et al. Parietofrontal network upregulation after motor stroke. *Neuroimage Clin*. 2018;18:720–729.